DNA AND CELL BIOLOGY
Volume 32, Number 12, 2013

Pp. 685–698
DOI: 10.1089/dna.2013.2032

Induction of Estrogen-Sensitive Epithelial Cells Derived from Human-Induced Pluripotent Stem Cells to Repair Ovarian Function in a Chemotherapy-Induced Mouse Model of Premature Ovarian Failure

Te Liu,[1,*] Wenxing Qin,[2,*] Yongyi Huang,[3,*] Yanhui Zhao,[4] and Jiejun Wang[2]

The incidence of premature ovarian failure (POF), a condition causing amenorrhea and hypergonadotropic hypoestrogenism in women before the age of 40, has been increasing in recent years. As an irreversible pathological change, improved treatment strategies for this disease are urgently needed. In this study, a type of microRNA (*miR-17-3p*) was used to guide the differentiation of human-induced pluripotent stem (iPS) cells into hormone-sensitive ovarian epithelial (OSE)-like cells *in vitro.* To prevent their morphological transformation into fibroblast-like cells, *MiR-17-3p*, a microRNA that suppresses *vimentin* expression, was transfected into human iPS cells. Subsequently, these cells were successfully induced into OSE-like cells *in vitro* after treatment with estrogen and cell growth factors. Compared with controls, iPS cells transfected with *miR-17-3p* expressed higher levels of epithelial markers (*cytokeratin 7*, *AE1*, *AE3*, and *E-cadherin*) and estrogen receptors (*ERα* and *ERβ*) while levels of mesenchymal markers (*fibronectin*, *vimentin*, and *N-cadherin*) lowered after the induction. The human iPS cell-derived OSE-like cells were then injected into cyclophosphamide-induced POF model mice to determine their potential benefit as grafts to repair ovarian tissues. The OSE-like cells survived within POF mouse ovaries for at least 14 days *in vivo*. Compared with the negative controls, expressions of *cytokeratin 7* and *ERβ* proteins were elevated while *fibronectin* and *vimentin* levels in ovarian tissues were downregulated in the OSE-like cell transplantation group. Moreover, the ovarian weight and plasma E_2 level increased over time in the transplantation with OSE-like cells, compared with control groups. Hence, we can draw the conclusion that iPS cells can be induced to differentiate into OSE-like cells *in vitro*.

Introduction

Premature ovarian failure (POF), also known as primary ovarian insufficiency (Persani *et al.*, 2010; McGuire *et al.*, 2011), occurs over a gradual and variable clinical course. This condition causes amenorrhea and hypergonadotrophic hypoestrogenism in women before the age of 40 (Duncan *et al.*, 1993; Bandyopadhyay *et al.*, 2003; Yucebilgin *et al.*, 2004; Goswami and Conway, 2005; Lee *et al.*, 2007; Rebar, 2008; Persani *et al.*, 2010; McGuire *et al.*, 2011). Approximately, 5% of women worldwide experience cessation of their menstrual cycle prior to age 40 as result of POF (McGuire *et al.*, 2011). In most cases, ovarian insufficiency occurs due to an anticipated depletion of the primordial follicular pool. The etiological causes that may activate such mechanisms are highly heterogeneous and may include chromosomal, genetic, autoimmune, metabolic, infectious, and iatrogenic factors. In addition, ovarian primordial follicular cells lack a sufficient capacity of regeneration, so that destruction of these cells may lead to ovarian dysfunction manifesting as POF (Yucebilgin *et al.*, 2004). Although the incidence of POF has increased in recent years, its origin remains largely unknown (Goswami and Conway, 2005; Persani *et al.*, 2010). Currently, POF is regarded as a condition that cannot be reversed, and improvements in treatment strategies over those currently available are urgently needed. Lee *et al.* (2007) have reported the impact of bone marrow transplantation on the

[1]Shanghai Geriatric Institute of Chinese Medicine, Longhua Hospital, Shanghai University of Traditional Chinese Medicine, Shanghai, China.
[2]Department of Medical Oncology, Shanghai Changzheng Hospital, Affiliated to The Second Military Medical University, Shanghai, China.
[3]School of Life Science and Technology, Tongji University, Shanghai, China.
[4]Shanghai Key Laboratory of Stomatology, Department of Oral and Cranio-maxillofacial Science, Shanghai Ninth People's Hospital, Shanghai JiaoTong University School of Medicine, Shanghai, China.
*These authors contributed equally to this work.

generation of immature oocytes and rescued long-term fertility in a preclinical mouse model of chemotherapy-induced POF. At the same time, Ghadami *et al.* used intraovarian injection of an adenoviral vector expressing the human follicle stimulating hormone (FSH) receptor to restore folliculogenesis in FSHR(−/−) FORKO mice for the treatment of POF (Ghadami *et al.*, 2010). Therefore, the use of cell transplantation for the treatment of POF shows promise as an effective therapeutical method.

Sensitive ovarian epithelial (OSE) cells also play a very important role in ovarian tissue repair and regeneration (Auersperg *et al.*, 2001; Gava *et al.*, 2008; Lawrenson *et al.*, 2009; Virant-Klun *et al.*, 2009, 2011; Mullany *et al.*, 2011). OSE cells are separated from the ovarian stroma by a layer of basement membrane and by the tunica albuginea, a dense collagenous connective tissue layer that gives the ovary a light color at the bottom (Auersperg *et al.*, 2001; Wong and Auersperg, 2003). Previous studies have indicated that OSE cells express many cell factors such as epidermal growth factor (EGF), basic fibroblast growth factor (bFGF), transforming growth factor β (TGF-β), lamina, human chorionic gonadotropin (hCG), interleukin (IL)-1/-6, several integrins and cadherins, and murine antigens such as MUC1 and 17β-hydroxysteroid dehydrogenase (Auersperg *et al.*, 2001). These cytokines can effectively promote ovarian tissue repair and regeneration (Auersperg *et al.*, 2001). In addition, several studies have shown that OSE cells can transport materials in and out of the peritoneal cavity and take part in the process of cyclical ovulatory rupture and repair by producing proteolytic enzymes (Auersperg *et al.*, 2001; Gava *et al.*, 2008; Mullany *et al.*, 2011; Virant-Klun *et al.*, 2011). Moreover, Bukovsky *et al.* have proved the existence of precursor pluripotent stem cells among OSE cells in human postmenopausal ovaries (Auersperg *et al.*, 2001). Based on the above evidences, it is persuasive to confirm the functions of OSE cells in maintaining and repairing ovarian tissue.

Stem cell transplantation therapies have been recommended as potential treatment for various irreversible conditions. Although pluripotent embryonic stem cells (ESCs) are ideal seed cells for transplantation, ethical issues regarding their source have restricted their application in cell therapies. In 2006, Takahashi and Yamanaka reported on the generation of induced pluripotent stem (iPS) cells from mouse fibroblasts by adding four transcription factors, Sox2, Oct4, Klf4, and c-Myc (Takahashi and Yamanaka, 2006). Since then, several other transcription factor combinations have been successfully tested (Liu *et al.*, 2012d). iPS cells share salient characteristics with ESCs but are generated via reprogramming of somatic cells through the forced expression of key transcription factors (Kiskinis and Eggan, 2010). Since iPS cells are not constrained by ethical concerns and are more readily available than ESCs, they hold great promise in regenerative medicine (Kiskinis and Eggan, 2010; Gardlik, 2012; Pan *et al.*, 2012; Russo and Parola, 2012). To date, transplantation of iPS cells has been studied in the laboratory to treat several conditions. Hanna *et al.* generated iPS cells from anemic mice, successfully differentiated them into hematopoietic progenitors, and subsequently transplanted these cells back into the anemic mouse, which resulted in substantially ameliorated pathological features of the disease (Hanna *et al.*, 2007; Kiskinis and Eggan, 2010). Others have reported therapeutic transplantation applications of iPS cells in mouse models of Parkinson's disease (PD), and iPS cell-derived dopaminergic neurons have been functionally integrated into the adult brain of a mouse model of PD, leading to an improvement of the phenotype (Wernig *et al.*, 2008; Xu *et al.*, 2009). Wernig *et al.* (2008) induced iPS cell differentiation into dopaminergic neurons *in vitro* for the first time, which were then transplanted into the brain of PD rat models. The experimental results revealed that iPS cells could be integrated into the striatum of the rat model and significantly reduce the typical PD symptoms of slow movements, stiff limbs, and tremors. Another study by Liu *et al.* (2011) showed that iPS cells derived from human skin fibroblast cells could be induced to differentiate into hepatocytes. Moreover, these cells were transplanted into livers of mice with cirrhosis, which showed significant therapeutic efficacy. In addition, when transplanted for the treatment of degenerative eye diseases, iPS cells have shown evidence of differentiating into retinal pigment epithelial cells in the eyes of patients with convoluted chorioretinal atrophy (Meyer *et al.*, 2011). Further, liver regeneration studies reported that iPS cell-derived hepatocytes could proliferate and improve liver function after their injection into liver blastocysts of chimeric mice (Espejel *et al.*, 2010; Russo and Parola, 2012). However, though use of iPS cells-derived normal seed cells or patient-specific cells is an advantage, use of iPS cells is still clinically not safe, especially when considering that they are produced through the insertion of factors, such as c-Myc, a factor known to be involved in the development of cancer.

In view of evidences outlined above, we decided to evaluate the potential application of iPS cells as seed cells to treat POF. Considering the function of OSE cells in ovarian tissue repair and regeneration, we aimed to induce the differentiation of iPS cells into estrogen-sensitive OSE-like cells and then test their therapeutic effects by injecting them into ovarian tissues of a mouse model of POF. Since generation of iPS cells using Yamanak four factors (Sox2, Oct4, c-Myc, and Klf4), the c-Myc and Klf4 factors were proto-oncogenes and these factors expressed highly in undifferentiated iPS cells rather than in differentiated cells. So, the use of differentiated instead of undifferentiated iPS cells would avoid potential teratoma formation *in vivo*. However, it was a challenge for us to control the differentiation of somatic cell-derived iPS cells into a specific type of cell, and fibroblast and epithelial cells almost always emerged simultaneously in this inducible system. *MicroRNA-17-3p* (*miRNA-17-3p*) has been shown to suppress the epithelial-to-mesenchymal transition of prostate cancer cells via inhibiting expression of the target *vimentin* gene (Zhang *et al.*, 2009; Dong *et al.*, 2011; Cheng *et al.*, 2012a). In this study, to investigate their feasibility in treating POF, estrogen-sensitive OSE-like cells were induced from *miRNA-17-3p*-transfected iPS cells with treatment of specific cytokines before transplantation into ovarian tissues of POF model mice.

Materials and Methods

Preparation of human amniotic epithelial cells

Human placentas were obtained with written and informed consent of pregnant women who were negative for HIV-I, hepatitis B, and hepatitis C. We were recognized by the Institutional Ethics Committee for an appropriate usage of human amnion. Amnion membranes were mechanically peeled from chorines of placentas obtained from women with an uncomplicated Cesarean section. The epithelial

layers with basement membrane attached were obtained and used to harvest human amniotic epithelial cells (HuAECs) as previously described with some modification (Liu *et al.*, 2012d). Briefly, the membrane was placed in a 250-mL flask containing DMEM medium and cut with a razor to yield 0.5–1.0 cm^2 segments. The segments were digested with 0.25% trypsin-EDTA (Invitrogen, Life Technologies Corporation) at 37°C for 45 min. The resulting cell suspension were seeded in a six-well plate in DMEM medium (Invitrogen) supplemented with 10% fetal calf serum (PAA Laboratories GmbH), penicillin (100 U/mL), and glutamine (0.3 mg/mL; Invitrogen) and incubated in a humidified tissue culture incubator containing 5% CO_2 at 37°C. The HuAECs grown to a density of about 100% were used as feeder layers for human iPS culture after mitomycin C (Sigma-Aldrich) treatment.

Coculture of human iPS cells with HuAECs

The human iPS cells were generated based on the description given in the previous article (Liu *et al.*, 2012d). iPS cultures were separated from the feeder cells by treatment with 0.125% trypsin–EDTA solution and cocultured with HuAECs. The cells were cultured in DMEM: F12 (1:1) medium supplemented with 15% KnockOut™ Serum Replacement and mixtured 1 mM sodium pyruvate, 2 mM L-glutamine, 0.1 mM nonessential amino acids, 0.1 mM beta-mercaptoethanol, and penicillin (25 U/mL)-streptomycin (925 mg/mL), but without leukemia inhibitory factor (LIF). All reagents were purchased from Invitrogen Life Technologies Corporation. Those cells were incubated in a humidified tissue culture incubator containing 5% CO_2 at 37°C. All cells were cultured on the same feeder until passage 10th before making ulterior experiments.

Recombinant lentivirus generation vector construction and cell transfection

All steps of recombinant lentivirus package were conducted according to the previously described protocol (Zhang *et al.*, 2009). The Lv2-*miR-17-3p* and Lv2-miR-mut lentivirus were built by Genepharma Corporation, the transfection of lentivirus was done according to the company's instructions. In brief, Co-transfection of human iPS cells was conducted using 4×10^7 PFU/mL Lv2-*miR-17-3p* or Lv2-miR-mut lentivirus, respectively, according to the manufacturer's protocol. The iPS cells were seeded in a six-well plate and cultured in DMEM: F12 (1:1) medium supplemented with 15% KnockOut Serum Replacement and mixtured 1 mM sodium pyruvate, 2 mM L-glutamine, 0.1 mM nonessential amino acids, 0.1 mM beta-mercaptoethanol, and penicillin (25 U/mL)-streptomycin (925 mg/mL) without LIF. All reagents were purchased from Invitrogen Life Technologies Corporation. Those cells were incubated in a humidified tissue culture incubator containing 5% CO_2 at 37°C and grown until a culture confluence of 80%.

Embryoid body formation and induced differentiation into the estrogen-sensitive OSE-like cells

The iPS cells were dissociated with 0.125% trypsin–EDTA solution and suspended onto Petri dishes with DMEM: F12 (1:1) medium supplemented with 15% KnockOut Serum Replacement and mixtured 1 mM sodium pyruvate, 2 mM L-glutamine, 0.1 mM nonessential amino acids, 0.1 mM beta-mercaptoethanol, and penicillin (25 U/mL)-streptomycin (925 mg/mL), but without LIF for 6 days. All reagents were purchased from Invitrogen Life Technologies Corporation. For the induction of differentiation into embryoid body (EB) cells, cells were cultured in induced cell-conditioned medium (DMEM: F12 (1:1) medium supplemented with 1% KnockOut Serum Replacement and mixtured 1 mM sodium pyruvate, 2 mM L-glutamine, 0.1 mM nonessential amino acids, penicillin (25 U/mL)-streptomycin (925 mg/mL), 5 mg/mL transferrin, 10 mg/mL insulin, 10 ng/mL human EGF, 10 ng/mL human bFGF, 1.0 U/mL of hGC, 50 ng/mL human FSH, 0.1 mmol human progesterone, 50 ng/mL human estradiol, and 10 ng/mL human TGF-β. All reagents were purchased from Invitrogen Life Technologies Corporation. Cells were incubated in a humidified tissue culture incubator containing 5% CO_2 at 37°C for 8 days.

RNA extraction and analysis by quantitative real-time polymerase chain reaction

Total RNA from each cell line was isolated with TRIzol Reagent (Invitrogen, Life Technologies Corporation), according to the manufacturer's protocol. The RNA samples were treated with DNase I (Sigma-Aldrich), quantified, and reverse-transcribed into cDNA with the ReverTra Ace- First Strand cDNA Synthesis Kit (TOYOBO, TOYOBO (SHANGHAI) BIOTECH CO., LTD.). Quantitative real-time polymerase chain reaction (qRT-PCR) was conducted with a RealPlex4 real-time PCR detection system from Eppendorf, with SyBR Green RealTime PCR Master Mix (TOYOBO, TOYOBO (SHANGHAI) BIOTECH CO., LTD.) as the detection dye. qRT-PCR amplification was performed over 40 cycles with denaturation at 95°C for 15 s and annealing at 58°C for 45 s. Target cDNA was quantified with the relative quantification method. A comparative threshold cycle (Ct) was used to determine gene expression relative to a control (calibrator), and steady-state mRNA levels are reported as an n-fold difference relative to the calibrator. For each sample, the maker gene Ct values were normalized with the formula $\Delta Ct = Ct\_genes - Ct\_18S\ RNA$. To determine relative expression levels, the following formula was used: $\Delta\Delta Ct = \Delta Ct\_all\_groups - \Delta Ct\_control\_group$. The values used to plot relative expressions of markers were calculated with the expression $2^{-\Delta\Delta Ct}$. The mRNA levels were calibrated on the basis of levels of *18S rRNA*. The cDNA of each gene was amplified with primers as previously described (Table 1) (Lawrenson *et al.*, 2009).

Luciferase report assay

All steps of luciferase report assay were conducted according to the previously described method (Zhang *et al.*, 2009, 2011; Wu *et al.*, 2010; Cheng *et al.*, 2011, 2012b; Liu *et al.*, 2012a). NIH-3T3 cells were seeded at a density of 3×10^4/well in 48-well plates and co-transfected with 400 ng of Lv2-*miR-17-3p* or Lv2-miR-mut vectors, 20 ng of pGL3-vim-3UTR-WT or pGL3-vim-3UTR-Mut, and pGL-TK (Progema) using Lipofectamine 2000 Reagent according to the manufacturer's protocol. After 48 h of transfection, luciferase activity was measured using the dual-luciferase reporter assay system (Progema).

RNA extraction and northern blotting analysis

In all groups, 20 μg total RNA of good quality was analyzed on a 7.5 M ureum 12% PAA denaturing gel and transferred to a Hybond N^+ nylon membrane (Amersham). Membranes

Table 1. Polymerase Chain Reaction Primer Sequences

Gene product	Forward (F) and reverse (R) primers (5′→3′)	Size (bp)
AE1	F: CTGCAGGACTTCACCAAGG	104
	R: TGGTCCTGAGTGTCCAGTTG	104
AE3	F: GTGGTCCAGAGCAGCAGGT	98
	R: GTTGTCCTCCAGTCGGTGAC	98
Cytokeratin 7	F: CTGCCTACATGAGCAAGGTG	108
	R: GGGACTGCAGCTCTGTCAAC	108
E-cadherin	F: TTGACGCCGAGAGCTACAC	93
	R: GACCGGTGCAATCTTCAAA	93
N-cadherin	F: GTGCATGAAGGACAGCCTCT	100
	R: CCACCTTAAAATCTGCAGGC	100
Fibronectin	F: CCATAAAGGGCAACCAAGAG	91
	R: ACCTCGGTGTTGTAAGGTGG	91
Vimentin	F: CTTCAGAGAGAGGAAGCCGA	97
	R: ATTCCACTTTGCGTTCAAGG	97
Estradiol Receptor-α	F: ATGATCAACTGGGCGAAGAG	93
	R: CAGGATCTCTAGCCAGGCAC	93
Estradiol Receptor-β	F: CATGATCCTGCTCAATTCCA	108
	R: ACCAAAGCATCGGTCACG	108
18s rRNA	F: CGTTGATTAAGTCCCTGCCCTT	202
	R: TCAAGTTCGACCGTCTTCTCAG	202

Table 2. The List of Primary Antibodies

Antibodies	Companies	Applications
Rabbit anti-*Cytokeratin 7*	Santa Cruz Technology	IF (1:200) WB (1:1000)
Rabbit anti-*Fibronectin*	Santa Cruz Technology	IF (1:200) WB (1:1000)
Rabbit anti-*Vimentin*	Santa Cruz Technology	IF (1:200) WB (1:1000)
Rabbit anti-*ERα*	Santa Cruz Technology	WB (1:1000)
Rabbit anti-*ERβ*	Santa Cruz Technology	IF (1:200) WB (1:1000)
Rabbit anti-Ki67	Chemicon	IF (1:200) WB (1:1000)
Rabbit anti-GAPDH	Cell Signaling Technology	WB (1:1000)

IF, immunofluorescence staining; WB, western blotting analysis.

were cross-linked using UV light for 30 s at 1200 mjoule/cm^2. Hybridization was performed with the *miR-17-3p* antisense starfire probe, 5′-CTACAAGTGCCTTCACTGCAGT-3′, the 22-nt *miR-17-3p* fragments were detected according to the instruction of the manufacturer. (Zhang *et al.*, 2009; Liu *et al.*, 2012b) After washing, membranes were exposed for 20–40 h to Kodak XAR-5 films (Sigma-Aldrich Chemical). As a positive control, all membranes were hybridized with a human U6 snRNA probe, 5′-GCAGGGGCCATGCTAATCTTCTCTG TATCG-3′. Exposure times for the U6 control probe varied between 15 and 30 min.

Western blotting analysis

Cells were lysed using a 2× loading lysis buffer (50 mM Tris–HCl, pH 6.8, 2% sodium dodecyl sulfate, 10% β-mercaptoethanol, 10% glycerol, and 0.002% bromophenol blue). The total amount of proteins from the cultured cells was subjected to 12% SDS-PAGE and transferred onto Hybrid-PVDF membrane (Millipore) membranes. After blocking with 5% (w/v) nonfat dried milk in TBST (Tris-buffered saline containing Tween-20; 25 mM Tris/HCl, pH 8.0, 125 mM NaCl, and 0.05% Tween-20), the PVDF membranes were washed four times (15 min each) with TBST at room temperature and incubated with primary antibody (Table 2). Following extensive washing, membranes were incubated with HRP-conjugated goat anti-rabbit IgG secondary antibody (1:1000; Santa Cruz Technology) for 1 h. After washing four times (15 min each) with TBST at room temperature, the immunoreactivity was visualized by enhanced chemiluminescence using ECL kit from Perkin-Elmer Life Science.

Immunofluorescence staining

The cultured cells were washed thrice with PBS and fixed with 4% paraformaldehyde (Sigma-Aldrich) for 30 min. After blocking, the cells were incubated first with primary polyclonal antibody (Table 2) overnight at 4°C, and then with FITC-conjugated goat anti-rabbit IgG antibody (1:200; Sigma-Aldrich) and 5 μg/mL DAPI (Sigma-Aldrich) at room temperature for 30 min. Then, the cells were thoroughly washed with TBST and viewed through a fluorescence microscope (DMI3000; Leica).

ELISA assay

The mouse estradiol (E_2) and FSH ELISA kit (Westang Bio) was used according to the protocol description to determine the level of E_2 or FSH in mouse plasma. Briefly, 100 μL of mouse E_2 or FSH standarded at concentrations of 8000, 4000, 2000, 1000, 500, 250, and 125 pg/mL or 10, 5, 2.5, 1.25, 0.625, 0.312, and 0.156 ng/mL or diluted mouse plasma were added to anti-E_2 or FSH antibody precoated microtest wells and incubated for 60 min. After washing thrice, the HRP-conjugated detection antibodies were added followed by substrate solution. The absorbance was determined at a wavelength of 450 nm.

The mouse model of POF and in vivo *xenograft experiments*

Hebetic female C57BL/6 mice ($n=96$), between 4 and 5 weeks of age, were obtained from the Shanghai Tongji University with Institutional Animal Care and Use Committer approval in accordance with institutional guidelines. All mice were maintained for 14 days, 3 to 4 per cage, in a temperature-controlled colony room under standard light–dark cycle with free access to food and water. The study protocol was in accordance with the article (Lee *et al.*, 2007). To create the POF model, mice had single intraperitoneal injection of 70 mg/kg cyclophosphamide (Sigma-Aldrich) at 6 weeks of age. Firstly, the animals ($n=64$) were divided into two groups: WT group ($n=32$) and POF group ($n=32$). At different time points (0, 7, 14, and 21 days), eight mice in each group were sacrificed using for ovarian weight, plasma E_2, and FSH testing. Next, the animals ($n=32$) were divided into four groups: Blank control group (eight animals of WT mouse), a negative control group (eight animals of POF

model) grafted with iPS-miR-mut in the right ovary, an experimental group (eight animals of POF model) grafted with iPS-*miR-17-3p* in the right ovary, and a vehicle group (eight animals of POF model) grafted with 10 μL PBS in the right ovary. One week after intraperitoneal cyclophosphamide injection, each experimental model mice received an injection of 10 μL of cells ($\sim 1 \times 10^3$ cell spheres/μL), which was harbored with a red fluorescence dye ($DiIC_{18}(3)$, 1′-dioctadecyl-3,3,3′,3′-tetramethylindocarbocyanine perchlorate), or PBS. The above steps were in accordance with the previously described method (Liu *et al.*, 2012c). The ulterior experiments of the animal models in both groups were conducted 7 days after the transplantation.

Statistical analysis

Each experiment was repeated at least thrice, and data were shown as the mean ± standard error where applicable; differences were evaluated with Student's *t*-test. A p value less than 0.05 was considered statistically significant.

Results

Characteristics of miR-17-3p *and its binding sites in the 3′-untranslated region of* vimentin *mRNA*

The precursor miRNA (pre-miRNA) sequence, mature miRNA sequence, chromosomal location and length of *miR-17-3p*, and the target *vimentin* gene were analyzed in multiple species using online research tools and the miRBase Target database (www.mirbase.org). Ten putative consecutive miRNA target sites were identified in the 3′-untranslated region (3′-UTR) of *vimentin* mRNA, depending on the species. In this study, we focused on the potential targeting sites within human *miR-17-3p* sequence in human *vimentin* 3′-UTR, which are conserved across species to varying degrees (Fig. 1A). To identify whether mature *miR-17-3p* could bind

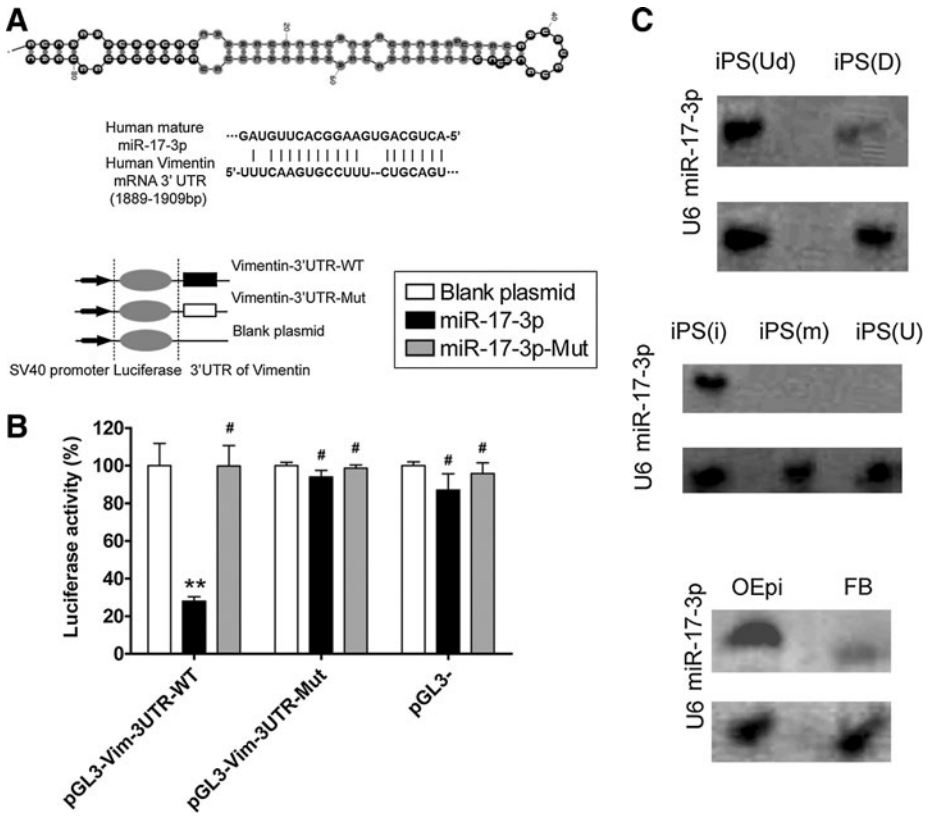

FIG. 1. Secondary structure of *miR-17-3p* and its expression in different cells. **(A)** Typical secondary structure of *hsa-miR-17-3p* precursor miRNAs (pre-miRNAs), contains stem-loop and hairpin structures, with a binding site located in an unstable region with a multi-branching loop-like RNA structure. Complementarity between *miR-17-3p* and the targeted human *vimentin* 3′-UTR site (1889–1909 bp downstream), and conserved bases of the mature *miR-17-3p* target sequence were present in the human *vimentin* 3′-UTR. **(B)** Expression of *miR-17-3p* and its effect on expression of the target gene *vimentin* was assessed by a luciferase assay. Wild-type (WT) reporter or mutated control luciferase plasmids were transfected into NIH-3T3 cells with *miR-17-3p* or *mut-miR-17-3p* expressing lentiviruses. Luciferase activity within the *vimentin* 3′-UTR sites was inhibited by *miR-17-3p* (**$p < 0.01$ vs. empty plasmid; $^{\#}p > 0.05$ vs. empty plasmid; $n = 3$). **(C)** Northern blotting results showing expression of *miR-17-3p* in different cells. In induced pluripotent stem (iPS) cells, a stronger *miR-17-3p* hybridization signal was observed in human iPS cells at the differentiated stage (D), compared with that at the undifferentiated stage (Ud). In transfected iPS cells, a stronger *miR-17-3p* hybridization signal was observed in human iPS cells transfected with the *miR-17-3p* expression plasmid (i), compared with those that were transfected with the mutant *miR-17-3p* (m) expression plasmid or were untransfected (U). In differentiated iPS cells, a stronger *miR-17-3p* hybridization signal was seen in ovarian epithelial-like cells derived from iPS cells (OEpi), compared with that in fibroblast cells (FB). *U6* RNA was used as a loading control in northern blot assays.

to sites in the *vimentin* mRNA 3′-UTR and further regulate its expression, an empty plasmid or plasmids expressing the 3′-UTR of wild-type (WT) or mutant *vimentin* was co-transfected with an expression vector for WT *miR-17-3p*, mutant *miR-17-3p* or corresponding empty vector into the mouse embryonic fibroblast cell line NIH-3T3. Luciferase activity with the *vimentin* 3′-UTR was significantly inhibited by WT *miR-17-3p* (mean ± SD, $p < 0.01$, $n = 3$), while that of the mutated *vimentin* 3′-UTR was not inhibited (Fig. 1B), suggesting that *miR-17-3p* targets *vimentin*. In addition, northern blotting was used to determine relative expression of *miR-17-3p* in different cells or in cells at different stages of induction. Only a mature *miR-17-3p* hybridization signal was observed in the undifferentiated stage of human iPS cells compared to the differentiated stage (Fig. 1C). A mature *miR-17-3p* hybridization signal was found in human iPS cells transfected with *miR-17-3p* but not in iPS cells transfected with the mutant *miR-17-3p* or in the untransfected group. Further, a mature *miR-17-3p* hybridization signal was only observed in estrogen-sensitive OSE-like cells but not in fibroblast cells derived from human iPS cells.

miR-17-3p-*transfected iPS cells express estrogen-sensitive OSE-like cell markers after induction*

Considering the risk of teratoma formation of transplanted undifferentiated iPS cells *in vivo*, these cells were first differentiated into somatic cells before transplantation (Fig. 2A). However, it was quite a challenge to control the differentiation of human iPS cells into a specific type of cell *in vitro*. Therefore, *miR-17-3p* was used to inhibit the expression of *vimentin* to limit the differentiation of human iPS cells into epithelial cells. First, the human iPS cells were divided into three groups. Two groups were either transfected with *miR-17-3p* or *miR-mut*, while the last group was untransfected. All cell groups were cultured in the same conditions. After EB cell formation, the three groups of cells were differentiated for 7 days. As observed by Hematoxylin and Eosin (H&E) staining to determine the cell morphology after induction, epithelioid-like cells gradually increased compared with the *miR-17-3p*-transfected iPS cells over the induction time *in vitro*. The vast majority of cells appeared polygonal with large nuclei and obviously stereoscopic by bright field microscopy (Fig. 2B). However, in the *miR-mut*-transfected and untransfected iPS cell groups, the cells displayed increasingly nonuniform morphology and consisted mostly of fibroblasts over the induction period. Moreover, these cells showed a slender spiral distribution and small nuclei, although a few epithelial cells were found interspersed in the heterogeneous population (Fig. 2B).

Next, to determine whether the induced cells above were estrogen-sensitive OSE-like cells, several cell markers were assayed by qRT-PCR, western blotting, and immunofluorescence (IF) staining. The qRT-PCR was used to compare the transcriptional levels of several important cell markers in each group, including epithelial markers (*cytokeratin 7*, *AE1*, *AE3*, and *E-cadherin*), mesenchymal markers (*fibronectin*, *vimentin*, and *N-cadherin*), and estrogen receptors (*ERα* and *ERβ*) after the iPS cells were induced to differentiate (Table 3). Relative mRNA expression was normalized to *18S rRNA*, which served as an internal control. Among the epithelial markers, *cytokeratin 7*, *AE3*, and *E-cadherin*, but not *AE1*, were expressed at significantly higher levels in the *miR-17-3p*-transfected iPS group than in the *miR-mut*-transfected iPS group or in the untransfected group (mean ± SD, $p < 0.01$, $n = 3$; Fig. 2C). However, the mesenchymal markers *fibronectin*, *vimentin*, and *N-cadherin* were expressed at significantly lower levels in the *miR-mut*-transfected iPS group or in the untransfected group. qRT-PCR analysis also showed that the *miR-17-3p*-transfected iPS group expressed the epithelial markers and the estrogen receptor *ERβ*.

In the *miR-17-3p*-transfected iPS group, western blotting revealed that levels of *cytokeratin 7* and *ERβ* protein were 2.095 ± 0.069 and 3.023 ± 0.043 of GAPDH expression levels, respectively (Fig. 2D). These values were significantly higher than those in the untransfected group (1.000 ± 0.123 and 1.000 ± 0.003 of GAPDH levels, respectively; mean ± SD, $p < 0.01$, $n = 3$). In contrast, the levels of *fibronectin* and *vimentin* expression in the *miR-17-3p*-transfected iPS group (0.261 ± 0.043 and 0.202 ± 0.048, respectively) were lower than those for the untransfected group (1.000 ± 0.146 and 1.000 ± 0.109 of GAPDH levels, respectively; mean ± SD, $p < 0.01$, $n = 3$). In addition, IF staining was performed 7 days after induction to compare the expression levels of epithelial markers, mesenchymal markers, and estrogen receptors in the *miR-17-3p*-transfected iPS group and *miR-mut*-transfected iPS group. Expression levels of *cytokeratin 7*, *ERβ*, and Ki-67 proteins were elevated in the *miR-17-3p*-transfected iPS group compared with those of the *miR-mut*-transfected iPS group (Fig. 3). However, *fibronectin* and *vimentin* protein levels were decreased in the *miR-17-3p*-transfected iPS group compared with those in the *miR-mut*-transfected iPS group after differentiation. These results suggest that when endogenous levels of *vimentin* are reduced by *miR-17-3p*, the iPS cells can differentiate into estrogen-sensitive OSE-like cells.

On the other hand, the ELISA assay was used to determine the estrogen responsiveness of the OSE-like cells *in vitro*. On days 1, 3, 5, 7, 9, and 11 after induction, the OSE-like cells culture medium were collected and were used for ELISA assay. We found the levels of estrogen in the cell culture medium of each group were not significantly different before induction (mean ± SD, $p > 0.05$, t test, $n = 3$). However, 5, 7, 9, and 11 days after induction, the levels of estrogen in the cell culture medium of each group significantly elevated in *miR-17-3p*-transfected iPS cells group (mean ± SD, $p < 0.01$, t test, $n = 3$), compared to the miR-mut group and untransfected group (Supplementary Fig. S1; Supplementary Data are available online at www.liebertpub.com/dna).

Establishment of a mouse model of chemotherapy-induced POF

To test our hypothesis above, we first established a mouse model of POF. Fourteen days after injection of chemotherapy drugs, the ovaries of POF model mice and normal healthy mice were collected and analyzed for pathologic analysis. Mouse plasma samples were collected to test the levels of the hormones E_2 and FSH in different groups. Histological results revealed that the ovaries of normal healthy mice contained a large number of follicles at all (from immature to mature) stages (Fig. 4B). In contrast, the atrophied ovaries of the POF model mice were mostly composed of interstitial

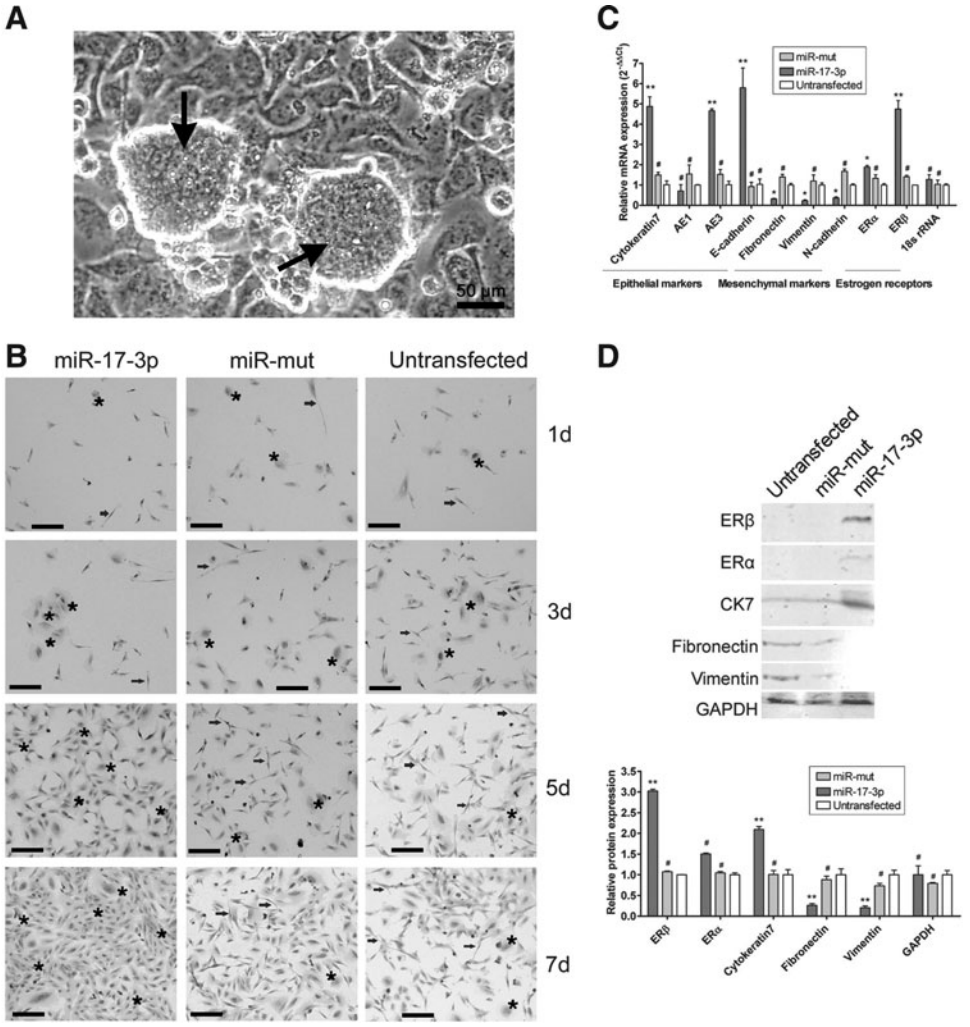

FIG. 2. Expression of multiple cell markers on differentiated cells derived from human iPS cells. **(A)** Human iPS cells (black arrows) were cultured on HuAECs feeder layers. Scale bar = 50 μm. Original magnification, 200×. **(B)** Morphological evaluation of cell groups (*miR-17-3p*-transfected iPS cells, *miR-mut*-transfected iPS cells, and untransfected cells) by H&E staining. Each cell group was induced to differentiate into somatic cells by specific hormones and cell growth factors over 7 days *in vitro*. The epithelioid-like cells (black stars) gradually increased in number as the *in vitro* induction time increased, compared with single in the *miR-17-3p*-transfected iPS cell group. However, in the *miR-mut*-transfected group and untransfected group, abundant fibroblast-like cells (black arrowheads) were present with fewer interspersed epithelioid-like cells. Scale bar = 50 μm. Original magnification, 200×. **(C)** Quantitative real-time polymerase chain reaction analysis of expression levels of epithelial markers (*cytokeratin 7*, *AE1*, *AE3*, and *E-cadherin*), mesenchymal markers (*fibronectin*, *vimentin*, and *N-cadherin*), and estrogen receptors (*ERα* and *ERβ*) after iPS cells were induced. The *miR-17-3p*-transfected group expressed epithelial markers and *ERβ*. Relative mRNA expression is shown after normalization to *18S rRNA*, serving as an internal control (**$p < 0.01$ vs. Untransfected; *$p < 0.05$ vs. Untransfected; $^{\#}p > 0.05$ vs. Untransfected; $n = 3$). **(D)** Western blotting showed *cytokeratin 7* and *ERβ* protein expression levels in the *miR-17-3p*-transfected iPS group were significantly higher than those of the untransfected group. However, *fibronectin* and *vimentin* expression levels in the *miR-17-3p*-transfected iPS group were lower than those of the untransfected group (**$p < 0.01$ vs. Untransfected; $^{\#}p > 0.05$ vs. Untransfected; $n = 3$).

cells in a fibrous matrix, with a reduced number of follicles at each stage. Additionally, ovaries of the POF model mice contained an increased number of atretic oocytes, while their uterine horns, ovaries, and fallopian tubes were reduced in size, compared with those of normal healthy mice (Fig. 4A). The weights of ovaries in the POF model mice were also obviously reduced compared with those in normal healthy mice (Table 4) (Fig. 4C). Plasma E_2 and FSH levels and ovarian pathology were investigated as well. After injection of cyclophosphamide, plasma E_2 levels decreased, while FSH levels increased over time in the POF mouse model group, but not in normal healthy mice. Results of these ELISA assays indicate that the POF model mice lack a hormonal maintenance from the ovaries (Table 5, Fig. 4D).

OSE-like cells survive and proliferate in ovaries of POF model mice

To investigate the treatment effect of transplanting OSE-like cells derived from iPS cells, red fluorescently (RF)-labeled iPS cell groups (*miR-17-3p*-transfected and *miR-mut*-transfected iPS groups) and the PBS control were injected

Table 3. Relative Expression of mRNAs in Different Groups ($2^{-\Delta\Delta CT}$)

	miR-17-3p-*transfected group* (n = 3)[a]	miR-mut-*transfected group* (n = 3)[b]	*Untransfected group* (n = 3)
Cytokeratin7	4.880 ± 0.472	1.491 ± 0.134	1.017 ± 0.185
AE1	0.702 ± 0.312	1.544 ± 0.442	1.000 ± 0.021
AE3	4.660 ± 0.097	1.524 ± 0.241	1.014 ± 0.171
E-cadherin	5.799 ± 0.975	0.922 ± 0.210	1.032 ± 0.256
Fibronectin	0.308 ± 0.031	1.396 ± 0.130	1.003 ± 0.073
Vimentin	0.229 ± 0.039	1.201 ± 0.294	1.004 ± 0.094
N-cadherin	0.366 ± 0.049	1.669 ± 0.121	1.001 ± 0.052
Era	1.881 ± 0.078	1.331 ± 0.174	1.002 ± 0.059
ERb	4.743 ± 0.426	1.406 ± 0.068	1.000 ± 0.003
18s rRNA	1.274 ± 0.231	1.035 ± 0.205	1.002 ± 0.055

[a] $p < 0.01$ versus Untransfected.
[b] $p > 0.05$ versus Untransfected.

into the ovaries of POF model mice (Fig. 5A), which were examined after 14 days to confirm the presence of transplanted cells. First, in the OSE-like cell (*miR-17-3p*-transfected iPS) transplantation group, pathological analysis of H&E-stained ovarian tissues showed that the number of atretic follicles was significantly reduced (mean ± SD, $p < 0.05$), but the number of mature follicles was increased (mean ± SD, $p < 0.05$; Fig. 5B). In contrast, both in the group transplanted with *miR-mut*-transfected iPS cells and in the PBS (vehicle) group, a larger number of atretic follicles were found in the ovarian tissues. The survival and proliferation of transplanted cells in the ovaries of POF model mice were determined. The BrdU IF assay showed that the BrdU-positive cells were elevated in ovaries of mice transplanted with OSE-like cells (Fig. 6), while BrdU-positive signals were hardly found by IF in the other two groups. As anticipated, RF-positive OSE-like cells could be observed along the injection tract after 14 days in the ovaries of POF model mice. These results demonstrated that the transplanted OSE-like cells could survive within the POF mouse ovaries for at least 14 days *in vivo*, and morphological changes could be seen thereafter. However, RF-positive *miR-mut*-transfected iPS

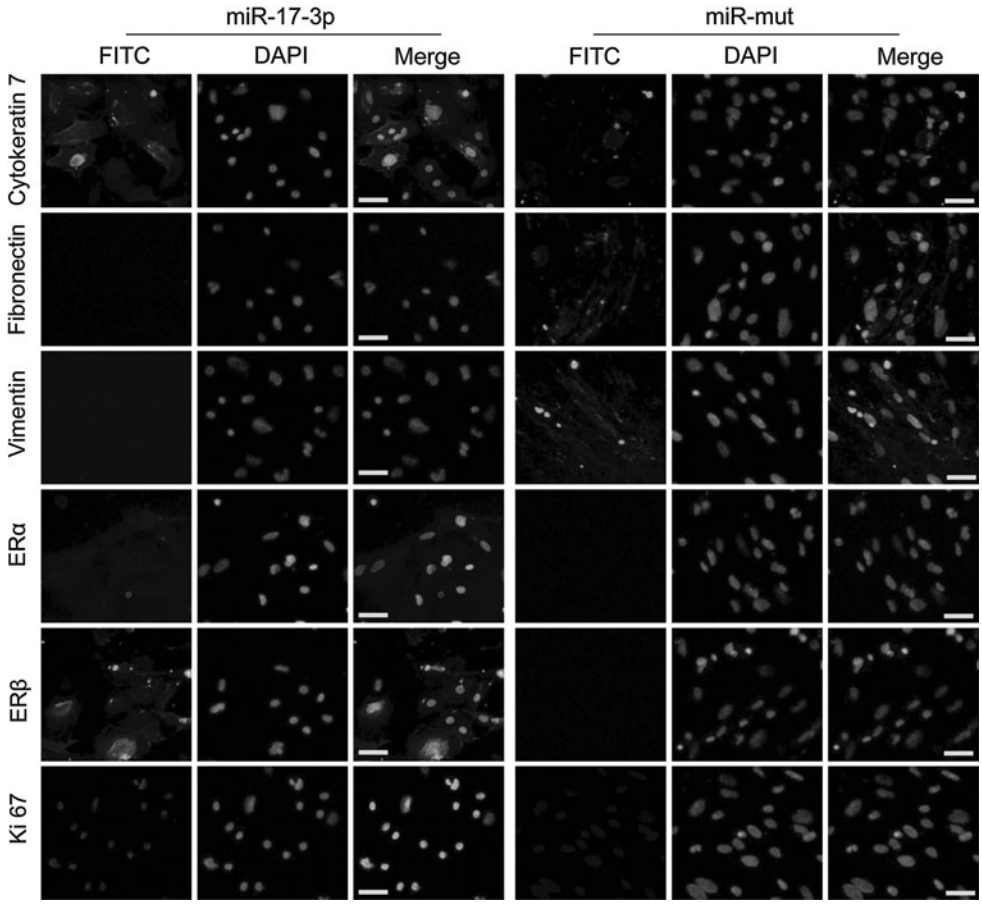

FIG. 3. IF staining of several ovarian epithelial cell markers on the 7th day after induction of iPS cells. Expression levels of *cytokeratin 7*, *ERβ*, and Ki-67 proteins were elevated in the *miR-17-3p*-transfected iPS group compared with the *miR-mut*-transfected iPS group. However, *fibronectin* and *vimentin* protein levels were decreased in the *miR-17-3p*-transfected iPS group compared with the *miR-mut*-transfected iPS group after differentiation. Scale bar = 50 μm. Original magnification, 200×. IF, immunofluorescence staining.

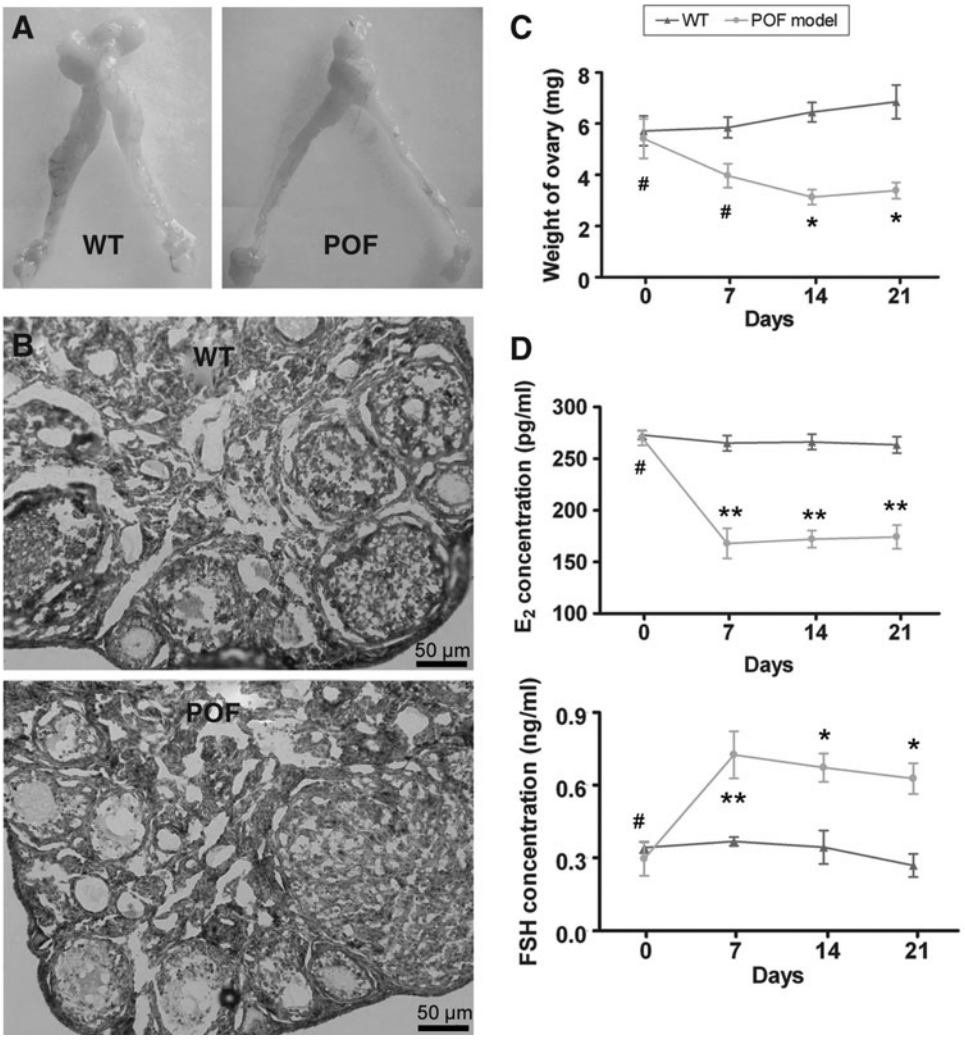

FIG. 4. Establishment of a premature ovarian failure (POF) mouse model and pathological analysis. **(A)** Female mouse reproductive system. **(A)** Fallopian tubes were narrowed and the ovaries were atrophied in POF mice model. **(B)** Pathological observation of ovaries from the WT group and POF group at 2 weeks after injection with cyclophosphamide. The atrophied ovaries of the POF model mice mostly consisted of interstitial cells in a fibrous matrix, with a reduced number of follicles at each stage and an increased number of collapsed oocytes. Scale bar = 50 μm. Original magnification, 200×. **(C)** The weight of ovaries in the POF model mice was found significantly reduced compared with that in normal healthy mice. $^{*}p < 0.05$ versus WT; $^{\#}p > 0.05$ versus WT. **(D)** Plasma E_2 levels and follicle stimulating hormone (FSH) levels determined by ELISA at various time points after the injection of cyclophosphamide. $^{**}p < 0.01$ versus WT; $^{\#}p > 0.05$ versus WT.

cells could not be found along the injection tract in the ovaries of POF model mice, confirming that only grafted OSE-like cells survived *in vivo*.

Further, IF staining was performed 14 days after transplantation to compare the expression levels of epithelial markers (*cytokeratin 7*), mesenchymal markers (*vimentin* and *fibronectin*), and estrogen receptors (*ERβ*) in ovarian tissues of each transplantation group. Expression levels of *cytokeratin 7* and *ERβ* proteins were elevated in ovarian tissues of mice transplanted with RF-positive OSE-like cells compared with those transplanted with RF-positive *miR-mut*-transfected iPS cells or PBS control (Fig. 6). However, expression levels of *fibronectin* and *vimentin* proteins were decreased in ovarian tissues of mice transplanted with RF-positive OSE-like cells compared to those transplanted with RF-positive *miR-mut*-transfected iPS or the PBS group. The results indicated that the OSE-like cells could improve ovarian fibrosis caused by POF after transplantation.

Transplanted OSE-like cells improve ovarian weight and hormone secretion in POF model mice

At 14 days after transplantation, the ovarian weight of each group was determined. The weight of ovaries in POF model mice transplanted with OSE-like cells obviously increased compared with those in the other two transplantation groups (Table 6). In addition, plasma E_2 and FSH levels were investigated by ELISA. The plasma E_2 level was elevated over time in the POF model mice transplanted with OSE-like cells compared with those in the other two groups (Table 6). However, among the three groups (OSE-like cell transplantation group, *miR-mut*-transfected iPS cell transplantation group, and PBS transplantation group), there was no significant difference in plasma FSH concentration (Fig. 7).

Table 4. Weights of Mice Ovaries

Time (Day)	*WT (mg)*	*POF model (mg)*
0	5.72 ± 0.59 ($n = 8$)	5.42 ± 0.77 ($n = 8$)[a]
7	5.85 ± 0.41 ($n = 8$)	3.97 ± 0.47 ($n = 8$)[a]
14	6.45 ± 0.38 ($n = 8$)	3.13 ± 0.30 ($n = 8$)[a]
21	6.85 ± 0.66 ($n = 8$)	3.38 ± 0.32 ($n = 8$)[a]

[a] $p < 0.05$ versus WT.
POF, premature ovarian failure; WT, wild-type.

Table 5. Plasma E_2 and Follicle Stimulating Hormone Levels

Time (Day)	E_2 (pg/mL)		FSH (ng/mL)	
	WT	POF model	WT	POF model
0	272.84 ± 4.24	270.22 ± 7.26	0.34 ± 0.02	0.30 ± 0.07
7	265.01 ± 7.44	167.89 ± 14.62[a]	0.37 ± 0.02	0.73 ± 0.10[a]
14	266.23 ± 7.43	172.04 ± 8.22[a]	0.34 ± 0.07	0.67 ± 0.06[b]
21	263.44 ± 7.94	174.21 ± 11.41[a]	0.27 ± 0.05	0.63 ± 0.06[b]

[a]$p < 0.01$ versus WT.
[b]$p < 0.05$ versus WT.
FSH, follicle stimulating hormone.

Discussion

The occurrence of POF has increased in recent years. Despite some treatments currently available for POF, it remains an irreversible disease awaiting improved treatment strategies. Research in regenerative medicine suggests that stem cells can be used to treat various human diseases, due to their self-renewal capacity and pleuripotent characters (Bandyopadhyay *et al.*, 2003; Goswami and Conway, 2005; Persani *et al.*, 2010; McGuire *et al.*, 2011). Therefore, it is reasonable to evaluate the feasibility of stem cells for the treatment of POF. While many lines of evidence have revealed great potentiation of iPS cell transplantation therapy in the treatment of various degenerative diseases, its utility in the treatment of POF remains to be evaluated. Despite much progress made in the generation and culture of iPS cells, the future of stem cell-based therapies and their productive use in drug discovery and regenerative medicine mainly depends on two key factors: maintaining the self-renewing capacity of multipotent and pluripotent cells and controlling their differentiation into desired derivatives *in vitro* or *in vivo*. However, although the iPS cells have the ability to differentiate into three germ layers, it still has the potential cancerous effects of transplanted undifferentiated iPS cells in body for a long term. Recently, Miura *et al.* (2009) induced evaluated the teratoma-forming propensity of secondary neurospheres generated from 36 mouse iPS cell lines derived in 11 different ways. After 55 mice transplanted with secondary neurospheres from 11 iPS cell clones derived from adult tail-tip fibroblasts, 46 mice died or became weak within 9 weeks after transplantation because of tumors. Besides, of 36 mice transplanted with seven iPS cell clones derived from hepatocyte, 13 died or became weak within 17 weeks after transplantation. And 10 of these mice developed tumors. Thus, secondary neurospheres from iPS cells derived from different adult tissues substantially varied in their teratoma-forming propensity, which correlated with the persistence of undifferentiated cells. four Yamanaka factors (Oct4, Sox2, Klf4, and c-Myc) have been used to induce the reprogramming of somatic cells into iPS cells (Takahashi and Yamanaka, 2006; Takahashi *et al.*, 2007). However, c-Myc and Klf4 are oncogenic factors, and previous studies indicate that

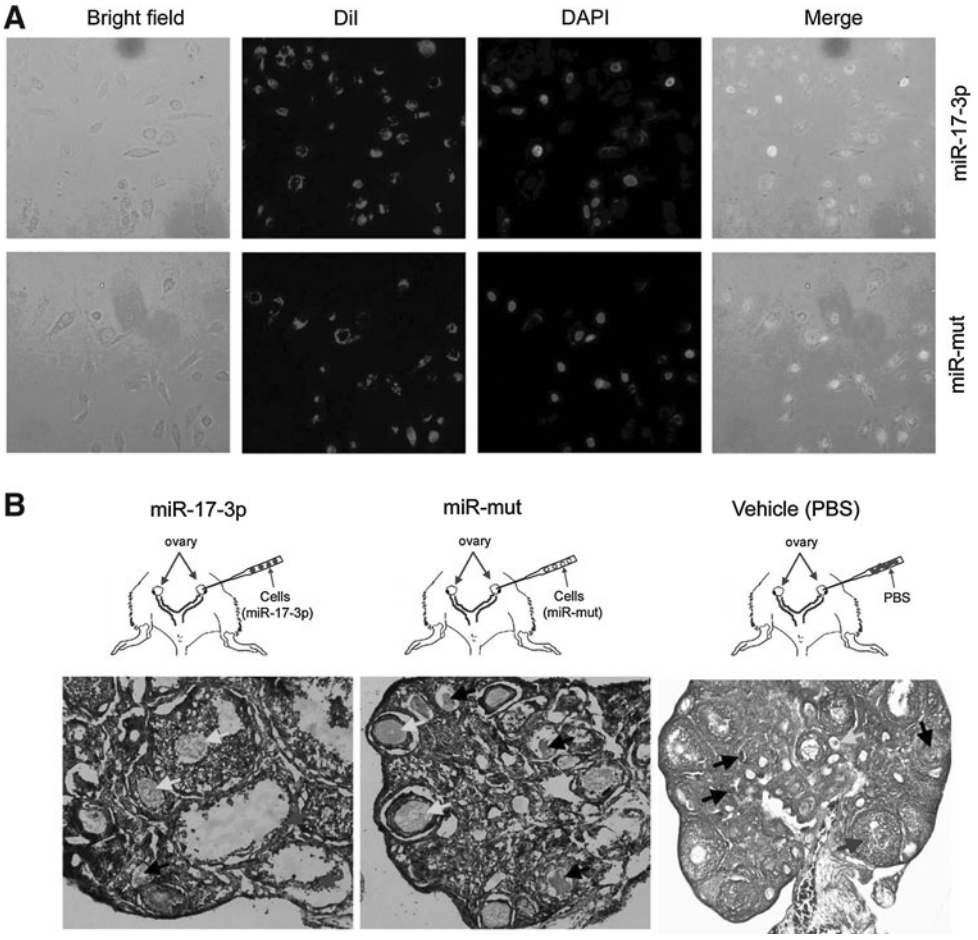

FIG. 5. Fluorescent dye of labeled cells transplanted into ovaries of POF model mice. **(A)** Each group of cells was labeled with the white fluorescent dye DiI *in vitro*. **(B)** H&E staining for pathological analysis of ovaries in each transplant group in POF model mice at 2 weeks after injection of iPS cells or PBS. Follicular atresia and ovarian fibrosis were significantly improved in the *miR-17-3p*-transfected iPS cells group but not in the *miR-mut*-transfected iPS cell transplantation group and vehicle group (PBS injected). The black arrows indicate the atretic follicles; white arrows indicate the mature follicles; gray arrows indicate the ovarian granulosa cells. Original magnification, 200×.

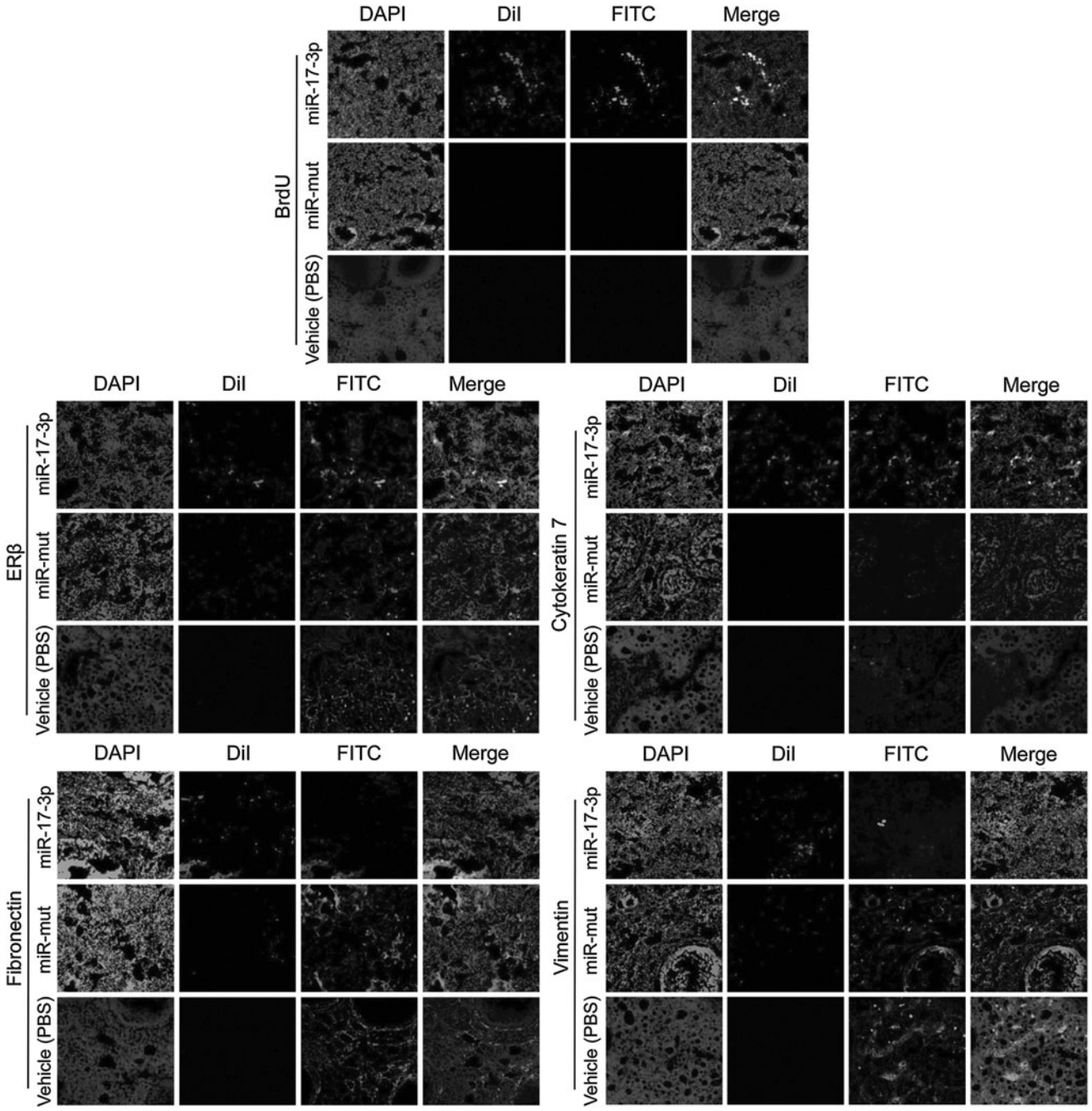

FIG. 6. Detection of specific biomarkers and hormone levels and ovarian weight change after cell transplantation. Survival of OSE-like cells in the ovary of a POF mouse model and changes in expression of specific biomarkers IF analysis demonstrated that DiI, a marker of transplanted cells, was expressed at higher levels in graft OSE-like cells in the mouse ovaries. The transplanted cells survived for at least 2 weeks *in vivo*. Moreover, BrdU incorporation and IF staining indicated that transplanted OSE-like cells had undergone normal cell division. However, in both the *miR-mut*-transfected iPS cell transplantation group and the vehicle group (PBS injected), DiI (white fluorescent, RF) and BrdU (white fluorescent) signals were not found. Thus, only OSE-like cells could be detected along the injection tract in POF mouse ovaries. Original magnification, 200×. In addition, *cytokeratin 7* and *ERβ* protein levels were elevated in ovarian tissues of the group transplanted with RF-positive OSE-like cells compared with those transplanted with miR-mut iPS cells or vehicle group (PBS injected). However, *fibronectin* and *vimentin* protein levels were decreased in ovarian tissues of the group transplanted with RF-positive OSE-like cells compared with the other two groups. Original magnification, 200×.

c-Myc might cause tumor development *in vivo* and Klf4 could induce tumor formation in offspring (Kim *et al.*, 2009; Wang *et al.*, 2009a, 2009b). Therefore, when iPS cells are used as seed cells to treat diseases, we must determine whether they have been differentiated fully *in vitro*. Otherwise, the risk of tumor occurring in acceptor's body will greatly increase with tumorigenicity of iPS cells. In this study, two crucial issues had to be addressed to obtain the desired effect by iPS cell transplantation in the treatment of POF. It is necessary not only to properly control the differentiation of

Table 6. Weights of Mice Ovaries and Plasma E_2 and Follicle Stimulating Hormone Levels After Cell Transplant

Mice	*OSE-like cells* (n = 8)	*iPS cells-miR-mut* (n = 8)	*Vehicle-PBS* (n = 8)	*WT* (n = 8)
Weight	5.33 ± 0.53[a]	4.29 ± 0.35	3.36 ± 0.34	6.23 ± 0.31[a]
E_2 (pg/mL)	222.08 ± 11.14[a]	162.31 ± 4.62	150.60 ± 4.28	260.24 ± 3.25[a]
FSH (ng/mL)	0.57 ± 0.04	0.62 ± 0.05	0.63 ± 0.04	0.27 ± 0.04[a]

[a]$p < 0.05$ versus Vehicle-PBS.
iPS, induced pluripotent stem.

iPS cells into hormone-sensitive ovarian epithelial-like cells (OSE-like cells) *in vitro*, but also to maintain long-term viability of these cells in the ovary. Typical changes of POF are ovarian atrophy and fibrosis; hormone secretions are thus affected by the increase in atretic follicles and decrease in mature follicles. Reversal of fibrosis and restoring normal hormone secretion are two key goals to effectively improve POF symptoms. In previous studies, OSE cells were proved to express many cell factors (Auersperg *et al.*, 2001), which could effectively promote ovarian tissue repair and regeneration. Therefore, a hypothesis is put forward that iPS cells may be induced to differentiate into estrogen-sensitive OSE-like cells, which can be transplanted into the ovaries for the treatment of POF.

In this study, to direct iPS cells toward becoming estrogen-sensitive OSE-like cells, *miR-17-3p* was used to suppress their differentiation into fibroblast-like cells *in vitro* by targeting the 3′-UTR sites of *vimentin*, thereby interfering with its expression. Estrogen and cell growth factors were used to induce the iPS cells to estrogen-sensitive cells. Because direct transplantation of iPS cells *in vivo* carries a risk of teratoma formation, the iPS cells had to be predifferentiated into somatic cells with proper physiological and biochemical functions *in vitro* before transplantation. This precaution provided a relatively safe protocol for the use of iPS cells *in vivo*. The combination of *miR-17-3p*, estrogen, and cell growth factors was shown to induce iPS cells to differentiate into estrogen-sensitive epithelial cells.

To verify the efficacy of OSE-like cell transplantation in the treatment of POF, a mouse model of chemotherapy-induced POF was established. In this disease model, the pathological changes of the mice were similar to those of POF patients, including atrophy of the ovaries and atretic follicles, which results in lowered E_2 and increased FSH. After ovary transplantation of OSE-like cells derived from human iPS cells, pathological analysis showed the relative reduction in atretic follicles and relative increase in mature follicles in the ovarian tissues in the transplanted group. Moreover, fibrotic cells in ovarian tissues were reduced while the weight of the ovaries increased. On the other hand, the most direct phenomenon of POF is the low expression of hormone E_2 and high expression of hormone FSH. In the ovary, the FSH stimulates the growth of immature follicles until the maturity of the Graafian follicle. However, follicles in the growth process can release inhibin to block further synthesis of FSH to ensure the selectivity of ovulation. The level of FSH, a direct reflection of the secretory function of ovaries, is a clinically important indicator of ovarian function. If level of FSH is too high, the reaction is ovarian secretion dysfunction. In addition, The E_2 can stimulate follicle development in ovary. The confusion of E_2 and FSH levels in POF model mice directly increased follicular dysplasia and follicular atresia. But, in this study, we found that the OSE-like cells might influence the observed increase in mature follicles and reduction in atretic follicles and decrease in fibrotic tissue because the ovarian function could be adjusted by the OSE-like cells. After OSE-like cells transplant into the ovaries of POF mice, originally reduced level of E_2 could rise again. Elevated E_2 could lead to the following results: (1) promotion of proliferation, differentiation, and maturation of ovarian epithelial cells and ovarian granulosa cells; (2) protection of primordial follicle pool and stimulation of follicular maturation and reduction of follicular atresia. In addition, E_2 level was also significantly higher in transplantation group, despite the lack of significance in FSH level difference before and after transplantation. In general, OSE cell transplantation provided

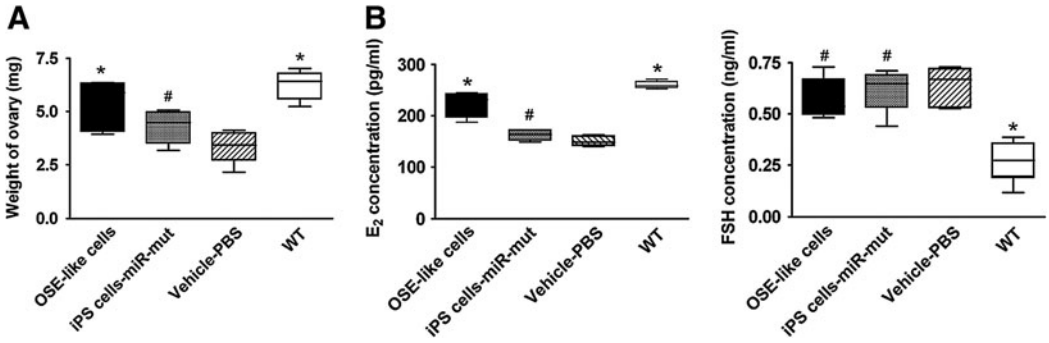

FIG. 7. Detection of hormone levels and ovarian weight after cell transplantation. **(A)** Ovarian weight in POF model mice transplanted with OSE-like cells increased significantly compared with that in the other two groups 14 days after transplantation (*$p < 0.05$ vs. vehicle group; #$p > 0.05$ vs. vehicle group; $n = 8$). **(B)** Plasma E_2 levels increased over time in the POF model mice transplanted with OSE-like cells compared with the other two groups. However, no significant difference in plasma FSH concentration was observed among the three groups (#$p > 0.05$ vs. vehicle group; $n = 8$).

benefits for symptom improvements in POF model mice. The controversy in plasma FSH level, as we speculate, derives from the manipulation of pituitary hormones, which prevent an obvious change in plasma levels of this hormone. Therefore, an artificial regulation of FSH expression would be a relatively complex and difficult goal to achieve.

The immunogenicity of iPS cells greatly enhanced after being induced into OSE-like cells *in vitro*. Theoretically, such somatic cells transplanted into mice should mediate an immune rejection, but absence of such phenomenon was observed in this study. We speculate that the use of chemotherapy drugs while establishing the POF mouse model may have led to an immune dysfunction with weakened reaction toward exogenous cells.

In conclusion, we evaluated the feasibility of iPS cell transplantation therapy in the treatment of POF. OSE-like cells derived from human iPS cells exerted certain positive effects on ovarian tissue morphology and function improvement in the mouse model of POF. Our study will open an array of new future investigations in human iPS cells transplanted to treatment in POF. This study has provided a new method of iPS cell transplantation in the treatment of POF disease. Moreover, this study will provide a guideline for efficient induction of the iPS cell differentiated into the ovarian tissue-like cells in future. In the next step, not only the epigenetic, genetic, and chromosomal stability of transplanted iPS cells, but also the long-term effect of transplanted iPS cells on the primordial follicle pool in this POF-induced mouse model will be investigated.

Acknowledgments

This work was supported by grants from the National Natural Science Foundation of China (No. 81202811) and the Shanghai Municipal Health Bureau Fund (No. 20124320) to Te Liu. We declare no potential conflict of interest.

Disclosure Statement

No competing financial interests exist.

References

Auersperg, N., Wong, A.S., Choi, K.C., Kang, S.K., and Leung, P.C. (2001). Ovarian surface epithelium: biology, endocrinology, and pathology. Endocr Rev **22,** 255–288.

Bandyopadhyay, S., Chakrabarti, J., Banerjee, S., Pal, A.K., Goswami, S.K., Chakravarty, B.N., *et al.* (2003). Galactose toxicity in the rat as a model for premature ovarian failure: an experimental approach readdressed. Hum Reprod **18,** 2031–2038.

Cheng, C.W., Wang, H.W., Chang, C.W., Chu, H.W., Chen, C.Y., Yu, J.C., *et al.* (2012a). MicroRNA-30a inhibits cell migration and invasion by downregulating vimentin expression and is a potential prognostic marker in breast cancer. Breast Cancer Res Treat **134,** 1081–1093.

Cheng, W., Liu, T., Jiang, F., Liu, C., Zhao, X., Gao, Y., *et al.* (2011). microRNA-155 regulates angiotensin II type 1 receptor expression in umbilical vein endothelial cells from severely pre-eclamptic pregnant women. Int J Mol Med **27,** 393–399.

Cheng, W., Liu, T., Wan, X., Gao, Y., and Wang, H. (2012b). MicroRNA-199a targets CD44 to suppress the tumorigenicity and multidrug resistance of ovarian cancer-initiating cells. FEBS J **279,** 2047–2059.

Dong, P., Kaneuchi, M., Watari, H., Hamada, J., Sudo, S., Ju, J., *et al.* (2011). MicroRNA-194 inhibits epithelial to mesenchymal transition of endometrial cancer cells by targeting oncogene BMI-1. Mol Cancer **10,** 99.

Duncan, M., Cummings, L., and Chada, K. (1993). Germ cell deficient (gcd) mouse as a model of premature ovarian failure. Biol Reprod **49,** 221–217.

Espejel, S., Roll, G.R., McLaughlin, K.J., Lee, A.Y., Zhang, J.Y., Laird, D.J., *et al.* (2010). Induced pluripotent stem cell-derived hepatocytes have the functional and proliferative capabilities needed for liver regeneration in mice. J Clin Invest **120,** 3120–3126.

Gardlik, R. (2012). Inducing pluripotency using *in vivo* gene therapy. Med Hypotheses **79,** 197–201.

Gava, N., C LC, Bye, C., Byth, K., and deFazio, A. (2008). Global gene expression profiles of ovarian surface epithelial cells *in vivo*. J Mol Endocrinol **40,** 281–296.

Ghadami, M., El-Demerdash, E., Salama, S.A., Binhazim, A.A., Archibong, A.E., Chen, X., *et al.* (2010). Toward gene therapy of premature ovarian failure: intraovarian injection of adenovirus expressing human FSH receptor restores folliculogenesis in FSHR(-/-) FORKO mice. Mol Hum Reprod **16,** 241–250.

Goswami, D., and Conway, G.S. (2005). Premature ovarian failure. Hum Reprod Update **11,** 391–410.

Hanna, J., Wernig, M., Markoulaki, S., Sun, C.W., Meissner, A., Cassady, J.P., *et al.* (2007). Treatment of sickle cell anemia mouse model with iPS cells generated from autologous skin. Science **318,** 1920–1923.

Kim, J.B., Sebastiano, V., Wu, G., Arauzo-Bravo, M.J., Sasse, P., Gentile, L., *et al.* (2009). Oct4-induced pluripotency in adult neural stem cells. Cell **136,** 411–419.

Kiskinis, E., and Eggan, K. (2010). Progress toward the clinical application of patient-specific pluripotent stem cells. J Clin Invest **120,** 51–59.

Lawrenson, K., Benjamin, E., Turmaine, M., Jacobs, I., Gayther, S., and Dafou, D. (2009). *In vitro* three-dimensional modelling of human ovarian surface epithelial cells. Cell Prolif **42,** 385–393.

Lee, H.J., Selesniemi, K., Niikura, Y., Niikura, T., Klein, R., Dombkowski, D.M., *et al.* (2007). Bone marrow transplantation generates immature oocytes and rescues long-term fertility in a preclinical mouse model of chemotherapy-induced premature ovarian failure. J Clin Oncol **25,** 3198–3204.

Liu, H., Kim, Y., Sharkis, S., Marchionni, L., and Jang, Y.Y. (2011). *In vivo* liver regeneration potential of human induced pluripotent stem cells from diverse origins. Sci Transl Med **3,** 82ra39.

Liu, T., Chen, Q., Huang, Y., Huang, Q., Jiang, L., and Guo, L. (2012a). Low microRNA-199a expression in human amniotic epithelial cell feeder layers maintains human-induced pluripotent stem cell pluripotency via increased leukemia inhibitory factor expression. Acta Biochim Biophys Sin (Shanghai) **44,** 197–206.

Liu, T., Cheng, W., Gao, Y., Wang, H., and Liu, Z. (2012b). Microarray analysis of microRNA expression patterns in the semen of infertile men with semen abnormalities. Mol Med Report **6,** 535–542.

Liu, T., Huang, Y., Guo, L., Cheng, W., and Zou, G. (2012c). CD44+/CD105+Human Amniotic Fluid Mesenchymal Stem Cells Survive and Proliferate in the Ovary Long-Term in a Mouse Model of Chemotherapy-Induced Premature Ovarian Failure. Int J Med Sci **9,** 592–602.

Liu, T., Zou, G., Gao, Y., Zhao, X., Wang, H., Huang, Q., *et al.* (2012d). High efficiency of reprogramming CD34(+) cells

derived from human amniotic fluid into induced pluripotent stem cells with Oct4. Stem Cells Dev **21,** 2322–2332.

McGuire, M.M., Bowden, W., Engel, N.J., Ahn, H.W., Kovanci, E., and Rajkovic, A. (2011). Genomic analysis using high-resolution single-nucleotide polymorphism arrays reveals novel microdeletions associated with premature ovarian failure. Fertil Steril **95,** 1595–1600.

Meyer, J.S., Howden, S.E., Wallace, K.A., Verhoeven, A.D., Wright, L.S., Capowski, E.E., *et al.* (2011). Optic vesicle-like structures derived from human pluripotent stem cells facilitate a customized approach to retinal disease treatment. Stem Cells **29,** 1206–1218.

Miura, K., Okada, Y., Aoi, T., Okada, A., Takahashi, K., Okita, K., *et al.* (2009). Variation in the safety of induced pluripotent stem cell lines. Nat Biotechnol **27,** 743–745.

Mullany, L.K., Fan, H.Y., Liu, Z., White, L.D., Marshall, A., Gunaratne, P., *et al.* (2011). Molecular and functional characteristics of ovarian surface epithelial cells transformed by KrasG12D and loss of Pten in a mouse model *in vivo*. Oncogene **30,** 3522–3536.

Pan, G., Wang, T., Yao, H., and Pei, D. (2012). Somatic cell reprogramming for regenerative medicine: SCNT vs. iPS cells. Bioessays **34,** 472–476.

Persani, L., Rossetti, R., and Cacciatore, C. (2010). Genes involved in human premature ovarian failure. J Mol Endocrinol **45,** 257–279.

Rebar, R.W. (2008). Premature ovarian "failure" in the adolescent. Ann N Y Acad Sci **1135,** 138–145.

Russo, F.P., and Parola, M. (2012). Stem cells in liver failure. Best Pract Res Clin Gastroenterol **26,** 35–45.

Takahashi, K., and Yamanaka, S. (2006). Induction of pluripotent stem cells from mouse embryonic and adult fibroblast cultures by defined factors. Cell **126,** 663–676.

Takahashi, K., Tanabe, K., Ohnuki, M., Narita, M., Ichisaka, T., Tomoda, K., *et al.* (2007). Induction of pluripotent stem cells from adult human fibroblasts by defined factors. Cell **131,** 861–872.

Virant-Klun, I., Rozman, P., Cvjeticanin, B., Vrtacnik-Bokal, E., Novakovic, S., Rulicke, T., *et al.* (2009). Parthenogenetic embryo-like structures in the human ovarian surface epithelium cell culture in postmenopausal women with no naturally present follicles and oocytes. Stem Cells Dev **18,** 137–149.

Virant-Klun, I., Skutella, T., Stimpfel, M., and Sinkovec, J. (2011). Ovarian surface epithelium in patients with severe ovarian infertility: a potential source of cells expressing markers of pluripotent/multipotent stem cells. J Biomed Biotechnol **2011,** 381928.

Wang, H., Wang, S., Hu, J., Kong, Y., Chen, S., and Li, L. (2009a). Oct4 is expressed in Nestin-positive cells as a marker for pancreatic endocrine progenitor. Histochem Cell Biol **131,** 553–563.

Wang, X., Zhao, Y., Xiao, Z., Chen, B., Wei, Z., Wang, B., *et al.* (2009b). Alternative translation of OCT4 by an internal ribosome entry site and its novel function in stress response. Stem Cells **27,** 1265–1275.

Wernig, M., Zhao, J.P., Pruszak, J., Hedlund, E., Fu, D., Soldner, F., *et al.* (2008). Neurons derived from reprogrammed fibroblasts functionally integrate into the fetal brain and improve symptoms of rats with Parkinson's disease. Proc Natl Acad Sci U S A **105,** 5856–5861.

Wong, A.S., and Auersperg, N. (2003). Ovarian surface epithelium: family history and early events in ovarian cancer. Reprod Biol Endocrinol **1,** 70.

Wu, S., Huang, S., Ding, J., Zhao, Y., Liang, L., Liu, T., *et al.* (2010). Multiple microRNAs modulate p21Cip1/Waf1 expression by directly targeting its 3′ untranslated region. Oncogene **29,** 2302–2308.

Xu, D., Alipio, Z., Fink, L.M., Adcock, D.M., Yang, J., Ward, D.C., *et al.* (2009). Phenotypic correction of murine hemophilia A using an iPS cell-based therapy. Proc Natl Acad Sci U S A **106,** 808–813.

Yucebilgin, M.S., Terek, M.C., Ozsaran, A., Akercan, F., Zekioglu, O., Isik, E., *et al.* (2004). Effect of chemotherapy on primordial follicular reserve of rat: an animal model of premature ovarian failure and infertility. Aust N Z J Obstet Gynaecol **44,** 6–9.

Zhang, L., Liu, T., Huang, Y., and Liu, J. (2011). microRNA-182 inhibits the proliferation and invasion of human lung adenocarcinoma cells through its effect on human cortical actin-associated protein. Int J Mol Med **28,** 381–388.

Zhang, X., Ladd, A., Dragoescu, E., Budd, W.T., Ware, J.L., and Zehner, Z.E. (2009). MicroRNA-17-3p is a prostate tumor suppressor *in vitro* and *in vivo*, and is decreased in high grade prostate tumors analyzed by laser capture microdissection. Clin Exp Metastasis **26,** 965–979.

Address correspondence to:
Te Liu, PhD
Shanghai Geriatric Institute of Chinese Medicine
Longhua Hospital
Shanghai University of Traditional Chinese Medicine
Shanghai 200031
China

E-mail: liute79@yahoo.com

Jiejun Wang, MD
Department of Medical Oncology
Shanghai Changzheng Hospital
Affiliated to The Second Military Medical University
Shanghai
China 200070

E-mail: jiejunw@csco.org.cn

Received for publication March 8, 2013; received in revised form August 10, 2013; accepted August 10, 2013.